

# SIZ1-mediated SUMOylation of CPSF100 promotes plant thermomorphogenesis by controlling alternative polyadenylation

Zhibo Yu<sup>1,4</sup>, Jun Wang<sup>1,4</sup>, Cheng Zhang<sup>1</sup>, Qiuna Zhan<sup>1</sup>, Leqian Shi<sup>1</sup>, Bing Song<sup>1</sup>, Danlu Han<sup>1</sup>, Jieming Jiang<sup>1</sup>, Junwen Huang<sup>1</sup>, Xiaolin Ou<sup>1</sup>, Zhonghui Zhang<sup>1</sup>, Jianbin Lai<sup>1,\*</sup>, Qingshun Quinn Li<sup>2,3,\*</sup> and Chengwei Yang<sup>1,\*</sup>

#### **ABSTRACT**

Under warm temperatures, plants adjust their morphologies for environmental adaption via precise gene expression regulation. However, the function and regulation of alternative polyadenylation (APA), an important fine-tuning of gene expression, remains unknown in plant thermomorphogenesis. In this study, we found that SUMOylation, a critical post-translational modification, is induced by a long-term treatment at warm temperatures via a SUMO ligase SIZ1 in *Arabidopsis*. Disruption of *SIZ1* altered the global usage of polyadenylation signals and affected the APA dynamic of thermomorphogenesis-related genes. CPSF100, a key subunit of the CPSF complex for polyadenylation regulation, is SUMOylated by SIZ1. Importantly, we demonstrated that SUMOylation is essential for the function of CPSF100 in genomewide polyadenylation site choice during thermomorphogenesis. Further analyses revealed that the SUMO conjugation on CPSF100 attenuates its interaction with two isoforms of its partner CPSF30, increasing the nuclear accumulation of CPSF100 for polyadenylation regulation. In summary, our study uncovers a regulatory mechanism of APA via SIZ1-mediated SUMOylation in plant thermomorphogenesis.

Key words: alternative polyadenylation, CPSF100, SIZ1, SUMOylation, thermomorphogenesis

Yu Z., Wang J., Zhang C., Zhan Q., Shi L., Song B., Han D., Jiang J., Huang J., Ou X., Zhang Z., Lai J., Li Q.Q., and Yang C. (2024). SIZ1-mediated SUMOylation of CPSF100 promotes plant thermomorphogenesis by controlling alternative polyadenylation. Mol. Plant. 17, 1392–1406.

#### INTRODUCTION

Global warming, which causes elevated ambient temperatures, has a profound influence on plant development (Hedhly et al., 2009). Warm ambient temperatures induce thermomorphogenesis in plants, such as leaf hyponasty, early fiowering, and elongation of hypocotyls, petioles, and roots, to overcome the effects of high temperatures (Casal and Balasubramanian, 2019). Downstream of the thermosensors, a transcription factor PHYTOCHROME INTERACTING FACTOR 4 (PIF4) acts as a central regulator in thermoresponses (Koini et al., 2009; Kumar et al., 2012). Multiple molecular mechanisms are involved in the control of plant thermoresponsive growth, including regulation processes in

transcription, alternative splicing, RNA metabolism, and protein stability (Quint et al., 2016; Hou et al., 2022).

mRNA polyadenylation is an essential co-transcriptional mechanism in the regulation of mRNA nuclear export, stability, and translation efficiency in eukaryotes (Tian and Manley, 2017). When the transcription of polymerase II reaches the end, nascent RNA is cleaved at its 3' end, followed by poly(A) tail synthesis via poly(A) polymerase. Importantly, more than 50% of eukaryotic genes

Published by the Molecular Plant Shanghai Editorial Office in association with Cell Press, an imprint of Elsevier Inc., on behalf of CSPB and CEMPS, CAS.

<sup>&</sup>lt;sup>1</sup>Guangdong Provincial Key Laboratory of Biotechnology for Plant Development, School of Life Science, South China Normal University, Guangzhou 510631, China

<sup>&</sup>lt;sup>2</sup>Key Laboratory of the Ministry of Education for Coastal and Wetland Ecosystems, College of the Environment and Ecology, Xiamen University, Xiamen, Fujian 361102, China

<sup>&</sup>lt;sup>3</sup>Biomedical Science Division, College of Dental Medicine, Western University of Health Sciences, Pomona, CA 91766, USA

<sup>&</sup>lt;sup>4</sup>These authors contributed equally to this article.

<sup>\*</sup>Correspondence: Jianbin Lai (20141062@m.scnu.edu.cn), Qingshun Quinn Li (liqq@xmu.edu.cn), Chengwei Yang (yangchw@scnu.edu.cn) https://doi.org/10.1016/j.molp.2024.07.011

use alternative poly(A) sites, called alternative polyadenylation (APA) (Wu et al., 2011; Shi, 2012; Fu et al., 2016, 2019). The choice of poly(A) sites is mediated by multiple protein complexes assembled at cis-elements around the 3' end region of pre-mRNAs (Shi and Manley, 2015). The cleavage and polyadenylation specificity factor (CPSF) complex, consisting of CPSF160, CPSF100, CPSF73, CPSF30, and FY, acts as a key complex in regulating APA via recognizing poly(A) signals in the near upstream elements (NUEs) or far upstream elements (FUEs) in Arabidopsis (Thomas et al., 2012; Lin et al., 2017; Yu et al., 2019; Song et al., 2021). Previous studies revealed that poly(A) factors are essential in the modulation of APA in plant development and stress tolerance (Deng and Cao, 2017; Téllez-Robledo et al., 2019; Ye et al., 2019; Conesa et al., 2020; Hunt, 2020; Wu et al., 2020; Yan et al., 2021; Kim et al., 2023; Lin and Li, 2023), but the regulatory mechanism and the molecular function of APA in plant thermomorphogenesis are unknown.

Post-translational modification (PTM) is a critical mechanism to rapidly change the functions of proteins during environmental stress response in plants (Niu et al., 2019; Han et al., 2022). SUMOylation is an important PTM that covalently attaches small ubiquitin-like modifiers (SUMOs) to lysine residues of substrates via an E1-E2-E3 enzyme cascade (Miura et al., 2007; Park et al., 2011). The levels of SUMO1/2 conjugates on diverse protein substrates are significantly increased in response to extreme heat stress (HS) in Arabidopsis, and this process is dependent on the SUMO E3 ligase SIZ1 (Kurepa et al., 2003). Previous works focused mostly on the molecular functions of SUMOylation in plant transcription regulation in extreme HS (Li et al., 2017; Wang et al., 2020; Zheng et al., 2022; Huang et al., 2023), but this modification is also involved in plant thermomorphogenesis under warm ambient temperatures. The sumo 1/2 knockdown mutant or the siz1-2 knockout mutant exhibits thermoinsensitivity at 28°C, but a short-term treatment at 28°C does not increase SUMO conjugates (Hammoudi et al., 2018). Although it has been determined that the SUMOylation of SEUSS positively regulates thermoresponsive hypocotyl elongation (Zhang et al.,2020), the underlying mechanism of SUMOylation in plant thermomorphogenesis remains unclear. Here, we uncovered a mechanism that shows that the SIZ1mediated SUMOylation of CPSF100 is essential for APA regulation in plant thermomorphogenesis.

#### **RESULTS**

Genome-wide alternative polyadenylation in response to warm temperatures is regulated by SIZ1

To reveal the mechanism by which SUMOylation regulates thermomorphogenesis in Arabidopsis, we confirmed the hypocotyl elongation phenotype of the *siz1-2* mutant at 28°C. Consistent with the previous report, the hypocotyl lengths of the *siz1-2* seedlings were significantly shorter than those in the wild type (WT; Figure 1A). A previous study showed that 28°C does not induce the accumulation of SUMO1/2 conjugates in a short time (Kurepa et al., 2003); thus, we treated the 5-day-old seedlings at 28°C for 1 or 4 days. Interestingly, compared to the 22°C control, the level of SUMO1/2 conjugates was significantly increased only after 1 day at 28°C in WT but not in *siz1-2* (Figure 1B and 1C), suggesting that the

SUMOylation is induced under this warm condition in a SIZ1-dependent manner.

Warm temperatures alter global gene expression (Hammoudi et al., 2018), but whether APA is involved in thermomorphogeneis mediated by SIZ1 remains unknown. Poly(A) tag sequencing (PAT-seq) was used to uncover the genome-wide profiling of poly(A) site usage, mature transcripts abundance, and functional gene expression in the Col-0 and siz1-2 mutant seedlings at 22°C and 28°C (Supplemental Figure 1 and 2A; Supplemental Table 1). In total, 65 971 poly(A) site clusters (PACs) were identified (Supplemental Data Set 1). These PACs were mapped to 22 112 genes, and 17 329 genes (78%) contained more than one PAC (defined as APA genes) (Supplemental Figure 2B). Over 70% of PACs were located at 3' UTRs, similar to previous results (Yu et al., 2019). Although the number of PAC distributions had no obvious differences between the 22°C and 28°C samples in either Col-0 or siz1-2 (Supplemental Figure 2C), poly(A) tags of PACs (the expression of transcripts) were increased in 3' UTRs but reduced in exons under 28°C; more interestingly, the deficiency of SIZ1 significantly enhanced this change (Figure 1D).

The QuantifyPoly(A) method, which employs usage ratios of each PAC per gene to evaluate APA dynamics (the genes with different usage ratios of each PAC in different temperatures were defined as switch genes), was then used to exclude the variations of PACs derived from transcription activation or repression (Ye et al., 2021). The results showed that 1171 and 1641 switch genes with different poly(A) site usages were differentially expressed in Col-0 and siz1-2, respectively, in response to 28°C (Supplemental Figure 2D). The depletion of SIZ1 specifically resulted in the alternation of poly(A) site usages of 950 switch genes. The heatmap analysis also showed that 28°C significantly changed the expression of these switch genes, and the expression patterns were varied in the Col-0 and siz1-2 plants (Supplemental Figure 2E). The further Gene Ontology (GO) analysis showed that these switch genes were associated with the response to stresses, such as temperature stimulus (Supplemental Figure 2F), gRT-PCR was used to verify the expression switch of APA transcripts of key regulators in thermomorphogenesis, including ELF3 (Thines and Harmon, 2010), YUC8 (Sun et al., 2012), PIF4 (Koini et al., 2009), and ELF4 (Tian et al., 2022), in the response to warm temperatures. Consistent with the PATseg data, compared to the WT, the depletion of SIZ1 promoted the expression of the proximal transcript in ELF3, YUC8, and PIF4, as well as the distal transcript in ELF4 under warm temperatures (Figure 1E). Overexpression of both proximal and distal PIF4 in WT significantly enhanced hypocotvl length at 22°C and 28°C. Notably, overexpression of distal PIF4 led to a more pronounced increase in hypocotyl growth at 28°C compared to proximal PIF4 (Figure 1F, 1G, and Supplemental Figure 3). Additionally, the luciferase (LUC) activity data showed that the expression of YUC8, an auxin biosynthesis gene for hypocotyl elongation, was suppressed more by the proximal transcript of ELF3 than the distal transcript of ELF3 (Figure 1H). Combined with the result that the usage ratio of the proximal transcript of ELF3 and PIF4 was increased in siz1-2 (Figure 1E), it provided an explanation of the hypocotyl elongation defect of siz1-2 under warm

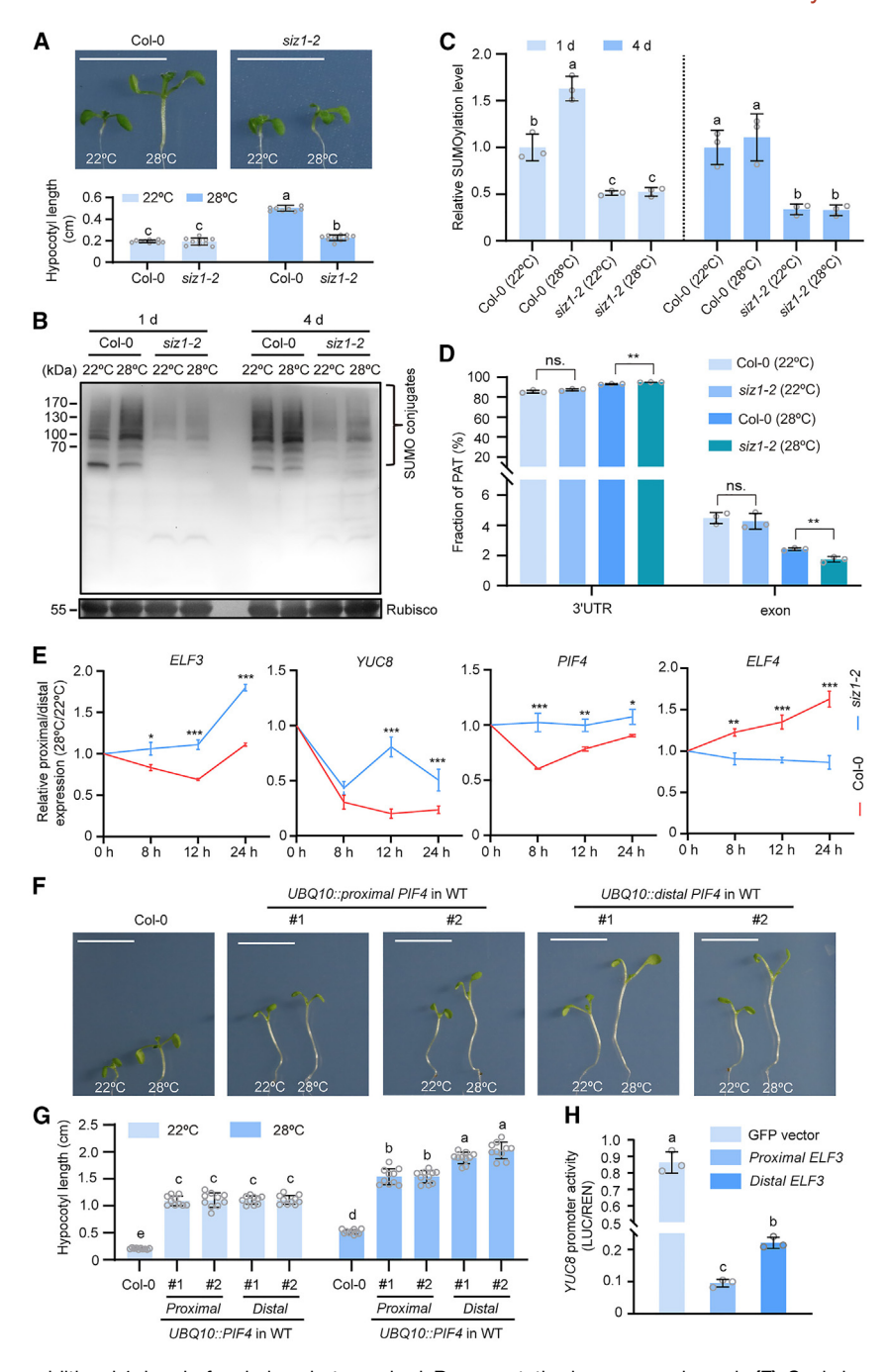


Figure 1. The genome-wide alternative polyadenylation in response to warm temperatures is regulated by SIZ1.

(A) Seedling phenotypes of Col-0 and siz1-2 grown at  $22^{\circ}$ C and  $28^{\circ}$ C. Seedlings were grown for 4 days at  $22^{\circ}$ C and then either kept at  $22^{\circ}$ C or transferred to  $28^{\circ}$ C for an additional 4 days before being photographed. The representative image is shown in the top graph. Scale bars, 1 cm. The quantitative data in the bottom graph are mean  $\pm$  SD (n=10) from one experiment. Three independent experiments showed similar patterns. Significant difference was analyzed via one-way ANOVA followed by Tukey's multiple comparisons test (p < 0.05).

**(B)** Five-day-old Col-0 and *siz1-2* seedlings were exposed to 28°C or 22°C for 1 or 4 days. Total proteins were extracted for immunoblotting with an anti-SUMO1 antibody. The loading controls from Coomassie blue staining are shown at the bottom. **(C)** Quantification of the SUMOylation levels in **(B)**. The SUMOylation signals in the immunoblots were quantified by ImageJ and modification levels were calculated from relative signals (SUMOylation Rubisco). The relative SUMOylation level of Col-0 at 22°C was set to 1. Data are mean ± SD from three biologically independent experiments. Significant difference was analyzed via one-way ANOVA followed by Tukey's multiple comparison tests (*p* < 0.05).

**(D)** The distributions of PATs in 3' UTR and exon regions. Significant difference was analyzed using Student's t test (\*\*p < 0.01; ns., p > 0.05).

**(E)** qRT-PCR analysis for the relative expression ratio of APA transcripts of *ELF3*, *YUC8*, *PIF4*, and *ELF4* in Col-0 and *siz1-2*. The relative expression of different transcripts was defined as the ratio of proximal transcript expression/distal transcript expression (28°C/22°C); the detailed calculation is included in Materials and methods. *ACTIN2* was used as an internal control. Data are mean  $\pm$  SD from three technological replicates in a single experiment. Three biologically independent experiments showed similar patterns. Significant difference between different samples at the same time point was analyzed using Student's t test (\*p < 0.05; \*\*\*p < 0.01; \*\*\*\*p < 0.001).

**(F and G)** The impact of overexpressing either the proximal or distal version of *PIF4* on hypocotyl elongation in response to warm temperatures. Seedlings were initially grown at 22°C for 4 days and then subjected to 22°C or 28°C for an

additional 4 days before being photographed. Representative images are shown in **(F)**. Scale bars, 1 cm. The quantification data of hypocotyl lengths of seedlings in **(G)** are mean  $\pm$  SD (n = 10) from a single experiment. Three biologically independent experiments showed similar patterns. Significant difference was analyzed via one-way ANOVA followed by Tukey's multiple comparisons test (p < 0.05).

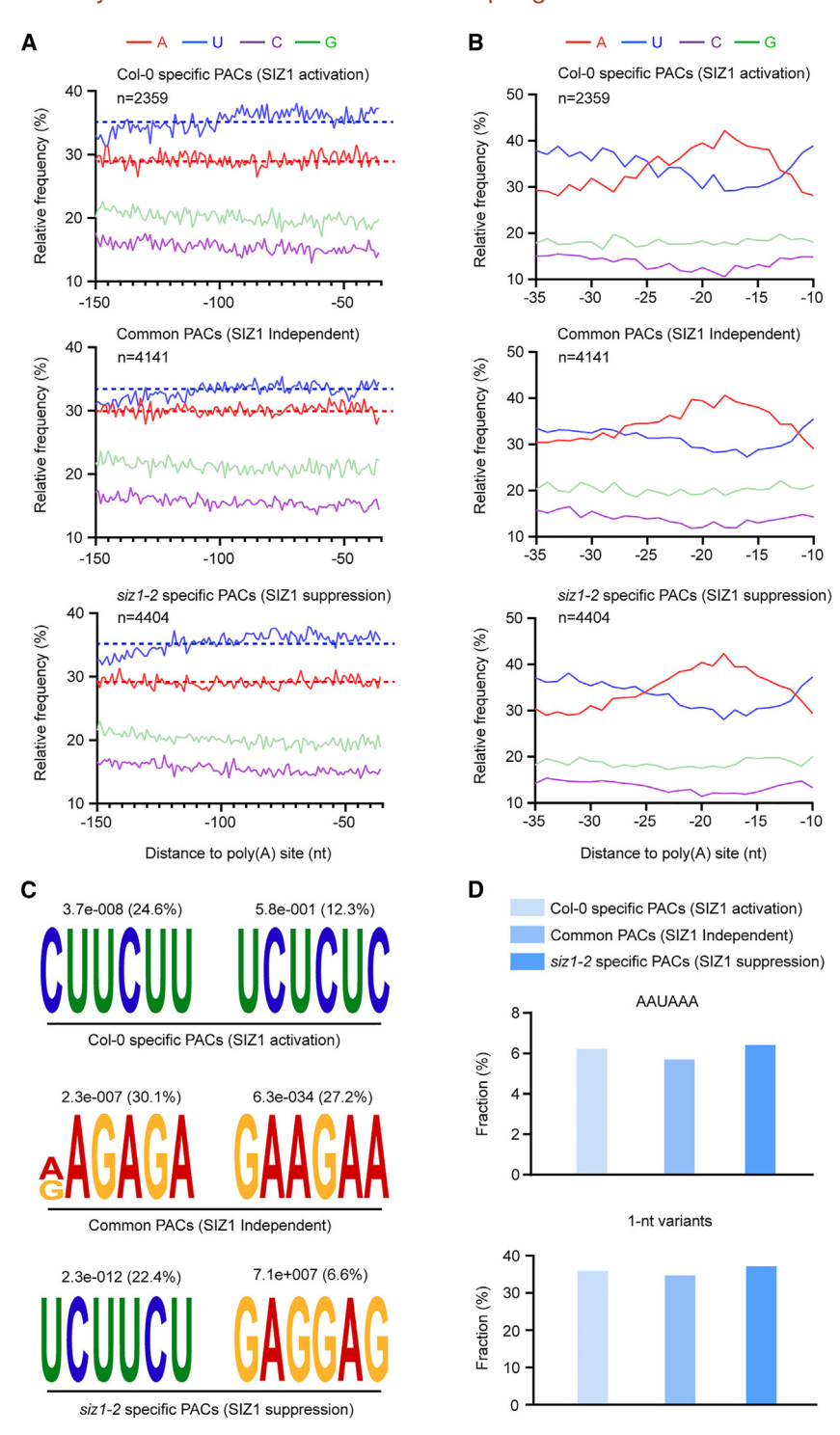
**(H)** The effect of the proximal and distal transcript of *ELF3* on the *YUC8* promoter activity. The GFP vector was used as a control sample. Data are mean  $\pm$  SD from three biologically independent experiments and significant difference were analyzed via one-way ANOVA followed by Tukey's multiple comparison tests (p < 0.05).

temperatures. Collectively, these data suggested that SIZ1 mediates APA in plant thermomorphogenesis.

## The deficiency of *SIZ1* alters the usage of poly(A) signals under warm temperatures

The usage of mRNA poly(A) sites is determined by the interaction between *cis*-elements on pre-mRNAs and a set of polyadenyla-

tion factors (Loke et al., 2005; Shi and Manley, 2015). To study these *cis*-elements, characterization of the single-nucleotide base compositions surrounding poly(A) sites was conducted in the NUEs and FUEs. The poly(A) sites were grouped into three sets: common PACs in Col-0 and *siz1-2* (SIZ1 independent), Col-0 specific PACs (SIZ1 activation), and *siz1-2* specific PACs (SIZ1 suppression). The frequency of U nucleotide usage in FUEs in SIZ1-regulated (activated and suppressed) PACs



was higher than that in common-regulated PACs (Figure 2A). There was also a similar trend in NUEs (Figure 2B). To identify poly(A) signals, we focused on A-rich NUE and U-rich FUE signals 10–35 and 36–150 nt upstream of PACs. More U-rich motifs in SIZ1-regulated PACs were used than in common PACs (Figure 2C). Furthermore, the frequency of the canonical poly(A) signal (AAUAAA) and its 1-nucleotide (1-nt) variants in NUEs was increased in SIZ1-regulated PACs (Figure 2D). These data supported that SIZ1 is associated with the usage of poly(A) signals in response to warm temperatures.

# Figure 2. The deficiency of *SIZ1* alters the usage of poly(A) signals under warm temperatures.

**(A)** Position-by-position analysis of average base composition in FUEs located -150 to -36 bp upstream of poly(A) sites in the Col-0 and *siz1-2* plants. The n represents the number of PACs used for the plot. The y axis indicates the fraction of nucleotide composition at x axis locations. The blue and red dotted lines represent the average frequency of U nucleotide usage and A nucleotide usage, respectively.

**(B)** Position-by-position analysis of average base composition in NUEs located -35 to -10 bp upstream of poly(A) sites in the Col-0 and siz1-2 plants. **(C)** Poly(A) signal motifs in FUEs identified by MEME. The motifs with the top 2 ratios (transcripts of enriched motifs/total transcripts) are shown. Enriched *E*-value and percentage are shown above each motif. **(D)** The AAUAAA signal usage and 1-nt variants of AAUAAA signal usage in NUEs. SIZ1 activation: Col-0 specific PACs; SIZ1 independent: common PACs in Col-0 and siz1-2; SIZ1 suppression: siz1-2 specific PACs.

# SUMOylation of CPSF100 is required for its function in plant thermomorphogenesis

Because SIZ1 contributes to APA in warm temperature responses, we screened the SUMOylation substrates involved in polyadenylation in a reconstituted system in bacteria cells (Supplemental Figure 4A). As a result, CPSF100, a key subunit of the CPSF complex, was identified as a SUMOylation substrate. Bioinformatics prediction (Zhao et al., 2014) indicated that the lysine residues K401. K412, and K491 of CPSF100 were potential SUMOylation sites (Figure 3A). Further biochemical data confirmed that all these lysine residues contributed to CPSF100 SU-MOylation (Supplemental Figure 4B), and the SUMO1 conjugations on CPSF100 were almost completely lost in the triple-site mutant (3KR: all three lysine residues were mutated to arginine residues) (Figure 3B).

SUMOylation of CPSF100 was then confirmed in plant cells via an immunoprecipitation (IP) assay. The WT CPSF100-GFP was covalently attached with SUMO1 at 22°C, and its

SUMOylation level was increased at 28°C; consistently, the SUMOylation level of the 3KR version of CPSF100-GFP was low in both conditions (Figure 3C and Supplemental Figure 5A). Furthermore, *in vivo* data showed that SUMOylation of CPSF100 was decreased in *siz1-2* at 22°C and 28°C (Figure 3D). Consistently, the overexpression of *SIZ1* resulted in increased SUMOylation of CPSF100 in plants (Supplemental Figure 5B).

Importantly, we found that the hypocotyls of *cpsf100* mutant seedlings were significantly shorter than those of WT at 28°C,

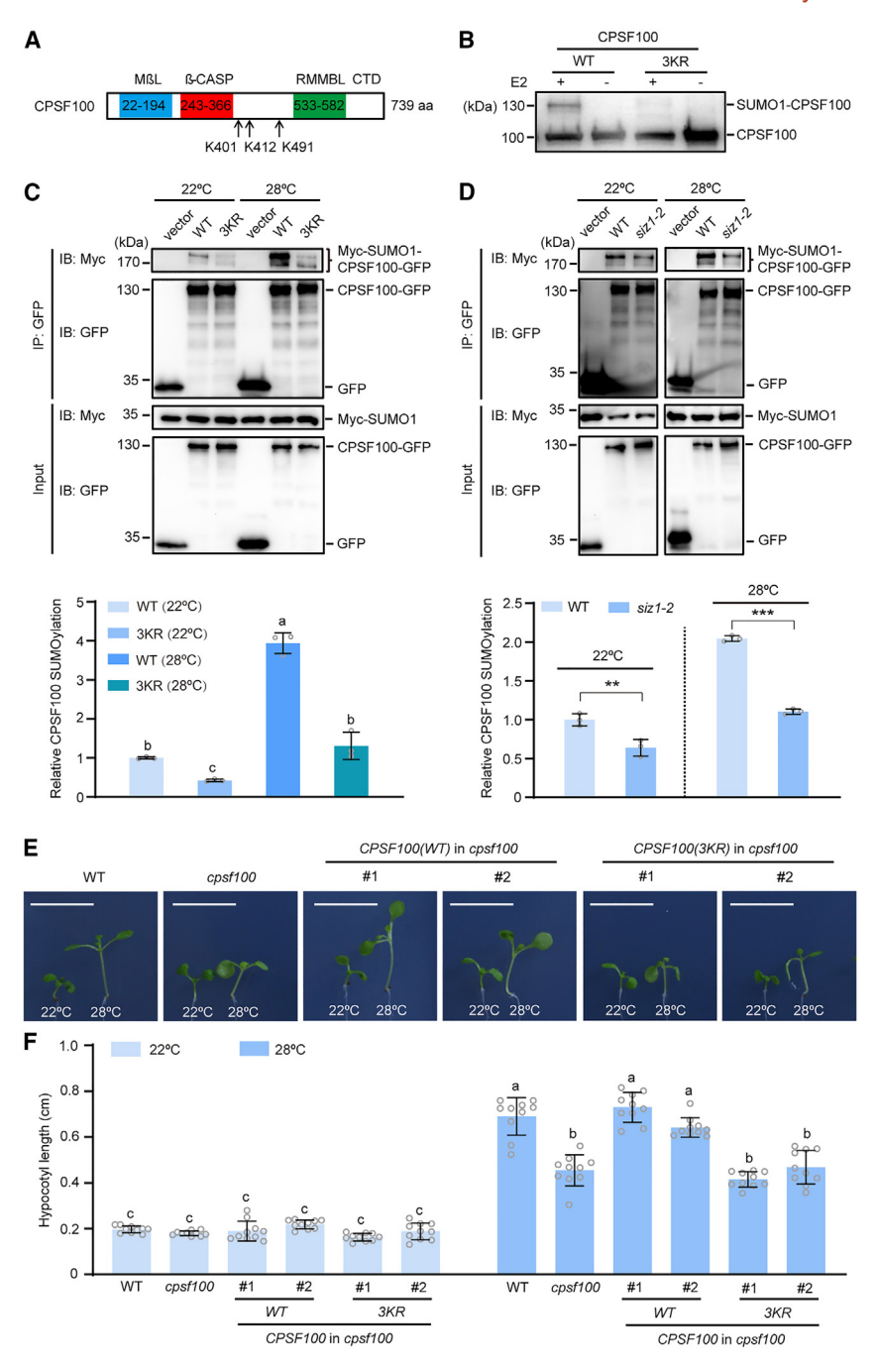


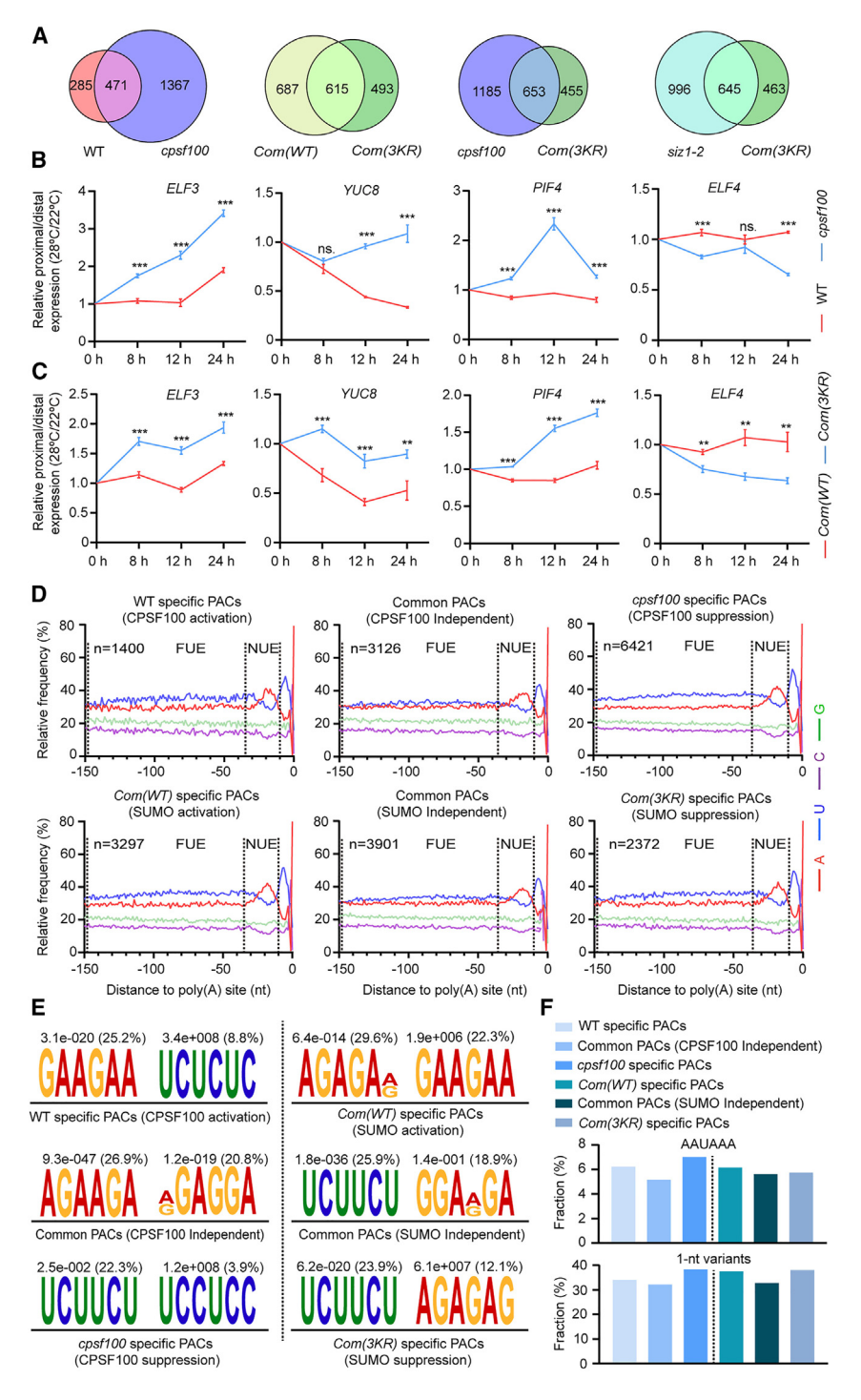
Figure 3. SUMOylation of CPSF100 is required for its function in plant thermomorphogenesis.

- (A) The predicted SUMOylation sites on CPSF100 using the GPS-SUMO Program. Three potential SUMOylation sites are indicated. The blue, red, and green regions represent the M $\beta$ L,  $\beta$ -CASP, and RMMBL domains, respectively.
- **(B)** Detection of CPSF100 SUMOylation in a reconstituted system in *E. coli*. In the presence of SUMO1GG and E1, the SUMOylation levels of the WT and 3KR (K401/412/491R) versions of CPSF100-FLAG with or without E2 (SCE1) were detected with an anti-FLAG antibody.
- (C and D) Determination of CPSF100 SUMOylation in plant cells. The WT or 3KR version of CPSF100-GFP was co-expressed with 5× Myc-SUMO1 in the WT protoplasts overnight at 22°C or 28°C (C). The WT CPSF100-GFP was co-expressed with 5× Myc-SUMO1 in the WT or siz1-2 protoplasts overnight at 22°C or 28°C (D). CPSF100-GFP was precipitated using anti-GFP beads. The input and pull-down samples were analyzed by immunoblots using anti-GFP and anti-Myc antibodies. The representative immunoblot images are shown in the top graphs; quantitative analysis of relative CPSF100 SUMOylation is shown in the bottom graphs. Data are mean ± SD from three independent experiments. Significant difference in (C) was analyzed via one-way ANOVA followed by Tukey's multiple comparison tests (p < 0.05); significant difference in (D) was analyzed via Student's t test (\*\*p < 0.01; \*\*\*p < 0.001).

**(E and F)** The seedling phenotypes of the WT, *cpsf100*, and the WT and 3KR versions of *CPSF100* complementary lines grown at 22°C and 28°C. Seedlings were grown for 4 days at 22°C and then either kept at 22°C or transferred to 28°C for an additional 4 days before being photographed. The representative images are shown in **(E)**. Scale bars, 1 cm. The quantification of hypocotyl lengths of seedlings in **(F)**. Data are mean  $\pm$  SD (n = 10) from one independent experiment. Three biologically independent experiments showed similar patterns. Significant difference was analyzed via one-way ANOVA followed by Tukey's multiple comparison tests (p < 0.05).

but similar to those of WT at 22°C (Figure 3E and 3F), supporting the role of CPSF100 in thermoresponsive hypocotyl elongation. However, the hypocotyls of *cpsf100* were similar to those of the WT in the dark, suggesting that it is specific to warm temperatures (Supplemental Figure 6A). Furthermore, the overexpression of *CPSF100* partially complemented the defect of hypocotyl growth in the *siz1-2* mutant in response to warm temperatures (Supplemental Figure 7), suggesting that SUMOylation of CPSF100 mediated by SIZ1 may be involved in the regulation of this process. To further determine the function of CPSF100 SUMOylation in thermomorphogenesis, the WT or 3KR version of CPSF100 under its native promoter was introduced into the *cpsf100* mutant. Independent transgenic lines

with similar *CPSF100* transcript levels (Supplemental Figure 8A) were selected for phenotype analysis. As a result, the *cpsf100* hypocotyl phenotype at 28°C was complemented by WT but not the 3KR variant of CPSF100 (Figure 3E and 3F), suggesting that SUMOylation is essential for the function of CPSF100 in plant thermomorphogenesis. Consistent with the previous report, the density and length of root hairs of the *cpsf100* mutant were found to be increased compared to those of the WT (Lin et al., 2017). Interestingly, this root hair phenotype of the *cpsf100* mutant was restored by either the WT or the 3KR variant of CPSF100 (Supplemental Figure 9). This result suggests that the 3KR variant of CPSF100 is functional in this process. These findings supported the notion that SUMOylation of



CPSF100 specifically regulates thermoresponsive hypocotyl growth.

## SUMOylation of CPSF100 mediates genome-wide poly(A) site choice under warm temperatures

To detect the effect of CPSF100 SUMOylation on genomewide poly(A) site choice in plant thermomorphogenesis, PATseq was used to uncover the poly(A) site usage and transcriptomic profiling of the WT, *cpsf100* mutant, and the WT and

# Figure 4. SUMOylation of CPSF100 mediates genome-wide poly(A) site choice under warm temperatures.

**(A)** The Venn diagrams for switch genes in the response to warm temperatures in the pairs of indicated plants. p < 0.05 was considered statistically significant for poly(A) sites' usage of switch genes. Com(WT), the WT version of CPSF100 complementary plants; Com(3KR), the 3KR version of CPSF100 complementary plants.

**(B and C)** qRT-PCR analysis for the APA expression of *ELF3*, *YUC8*, *PIF4*, and *ELF4* in the WT and *cpsf100* **(B)**, and the WT and 3KR versions of *CPSF100* complementary lines **(C)** at 22°C and 28°C. The relative expression of different transcripts was defined as the ratio of proximal transcript expression/distal transcript expression (28°C/22°C); the detailed calculation is included in Materials and methods. Data are mean  $\pm$  SD from three technological replicates in a single experiment. Three biologically independent experiments showed similar patterns. Significant difference between different samples at the same time point was analyzed using Student's t test (\*\*p < 0.01; \*\*\*p < 0.001; ns., p > 0.05).

**(D)** Position-by-position analysis of average base composition at 150 nt upstream of poly(A) sites, including FUEs and NUEs, in the WT, *cpsf100*, and complementary plants. n represents the number of PACs used for the plots. The y axis indicates the fraction of nucleotide composition at x axis locations.

**(E and F)** The FUE and NUE analysis in WT, *cpsf100*, and complementary plants. Poly(A) signal motifs in FUEs identified by MEME are shown in **(E)**. The motifs with top two ratios (transcripts of enriched motifs/total transcripts) are shown. Enriched *E*-value and percentage are shown above each motif. The AAUAAA signal usage and 1-nt variants of AAUAAA signal usage in NUEs are shown in **(F)**.

3KR versions of *CPSF100* complementary lines at 22°C and 28°C (Supplemental Table 1). Quantification of APA dynamics revealed that 756 and 1838 switch genes with different poly(A) site usages were differentially expressed in the WT and *cpsf100* mutant in response to 28°C, respectively (Figure 4A). Compared with those of the WT *CPSF100* complementary plants, over 40% of switch genes were specific in the 3KR version of *CPSF100* comple-

mentary plants. Interestingly, over 35% of switch genes in the *cpsf100* mutant overlapped those in the 3KR version of *CPSF100* complementary plants (Figure 4A). In addition, over 40% switch genes in *siz1-2* were found to be overlapped with those in *CPSF100(3KR)* complementary plants (Figure 4A), This suggests that the role of SIZ1 in regulating APA in plant thermomorphogenesis is mediated by the SUMOylation of CPSF100. GO analysis showed that these switch genes were also involved in response to stresses, including temperature stimulus (Supplemental Figure 10). We also found that some

#### **Molecular Plant**

switch genes are associated with auxin signaling and gibberellin signaling (Supplemental Data Set 2), which may be involved in thermomorphogenesis. Consistently, the APA dynamic patterns of *ELF3*, *YUC8*, *PIF4*, and *ELF4* in the comparison between WT and 3KR versions of *CPSF100* complementary plants were similar to those in the WT and *cpsf100* comparison (Figure 4B and 4C). Overall, these data supported that SUMOylation of CPSF100 mediates APA in response to warm temperatures.

Characterization of single-nucleotide base compositions surrounding poly(A) sites was also performed in these plants. The increase in A/U nucleotide usage in NUEs and U nucleotide usage in FUEs was found in CPSF100-regulated PACs and CPSF100 SUMOylation-regulated PACs, compared with the common PACs, respectively (Figure 4D). More U-rich motifs in FUEs were used in the CPSF100-regulated PACs. However, more U-rich motifs in FUEs were found only in CPSF100 SUMOylation-suppressed PACs, but not in CPSF100 SUMOylation-activated PACs (Figure 4E). We speculated that more common PACs overlapped in the WT and 3KR versions of CPSF100 complementary plants, leading to the increase in U-rich signals in common PACs. Interestingly, the usage frequency of canonical poly(A) signal AAUAAA and 1-nt variants in NUEs was also increased in CPSF100-regulated PACs and CPSF100 SUMOylationregulated PACs (Figure 4F). These data provided evidence for the notion that SUMOylation of CPSF100 regulates APA by modulating the usage of the poly(A) signals under warm conditions.

## SUMOylation of CPSF100 suppresses its interaction with CPSF30 isoforms

Because SUMOylation may alter substrate distribution in different subcellular compartments, the effect of SUMO on CPSF100 localization was analyzed. Interestingly, the cytoplasmic accumulation of CPSF100 was increased in siz1-2 and the 3KR version of CPSF100 complementary plants, compared to WT at 22°C and 28°C (Figure 5A and Supplemental Figure 11). Previous studies demonstrated that CPSF30, another subunit of the CPSF complex, enhances the translocation of CPSF100 from the nucleus to the cytoplasm (Rao et al., 2009). Therefore, we examined whether SUMOylation of CPSF100 has a dynamic effect on its interaction with CPSF30. Three isoforms of CPSF30 proteins were expressed in Arabidopsis, including CPSF30-S (28 kDa), CPSF30-M (45 kDa), and CPSF30-L (70 kDa) (Supplemental Figure 12). The previous study showed that CPSF30-S is associated with CPSF100 (Zhao et al., 2009). The co-IP data confirmed that all three isoforms of CPSF30 proteins were the interacting partners of CPSF100 in plant cells; however, mutation of SUMOylation sites of CPSF100 increased its association with CPSF30-M and CPSF30-L, but did not affect its interaction with CPSF30-S at both 22°C and 28°C. Consistently, CPSF100 increased its association with CPSF30-M and CPSF30-L in siz1-2 mutant (Figure 5B-5F and Supplemental Figure 13). The effect of SUMOylation of CPSF100 on its interaction with CPSF30-M and CPSF30-L was confirmed in a LUC complementation imaging (LCI) assay (Supplemental Figures 14 and 15). Consistently, the association between

#### SUMOvlation controls APA in thermomorphogenesis

CPSF100 and CPSF30-M was weakened by SIZ1 overexpression in Nicotiana benthamiana leaves (Supplemental Figure 16). Given that CPSF30-S and CPSF30-M were predominantly localized in the cytoplasm while CPSF30-L was mainly localized in the nucleus (Supplemental Figure 17), CPSF30-M may predominantly contribute to the translocation of SUMOylation-defective CPSF100 from the nucleus to the cytoplasm. Thus, we further compared the subcellular localization of the WT and 3KR versions of CPSF100-GFP with the overexpression of CPSF30-M in a nuclear fractionation assay. In this situation, the percentage of SUMOylation-defective CPSF100-GFP in the cytoplasm was significantly higher than its WT form, possibly resulting from its stronger interaction with CPSF30-M for maintenance in the cytoplasm (Figure 5G). Interestingly, although CPSF30-L was predominantly localized in the nucleus, its effect on the SUMOylation-regulated translocation of CPSF100 was similar to CPSF30-M (Supplemental Figure 15C), which may be contributed by the small population of CPSF30-L in the cytoplasm. Collectively, these data supported that SUMOylation of CPSF100 is important for its interaction with CPSF30 isoforms and its subcellular localization.

## CPSF30 modulates global poly(A) site usage in thermomorphogenesis

Because CPSF30-M and CPSF30-L modulate the subcellular localization of CPSF100 in a SUMOylation-dependent manner under warm temperatures, the role of CPSF30 in thermorphogenesis was also investigated. It was found that the cpsf30 mutant showed shorter hypocotyl elongation compared to Col-0 under 28°C (Figure 6A and 6B). The defect of hypocotyl elongation in cpsf30 is also specific to warm temperatures (Supplemental Figure 6). Then, three isoforms of CPSF30 driven by the native promoter were introduced into cpsf30 plants and the transgenic lines with similar expression levels were used for phenotype analysis (Supplemental Figure 8B). Consistently, the hypocotyl elongation defect of cpsf30 at 28°C was complemented by CPSF30-L or CPSF30-M, but not by CPSF30-S (Figure 6A and 6B), supporting the idea that CPSF30-L and CPSF30-M are required for thermoresponsive hypocotyl elongation.

PAT-seq was then used to uncover the poly(A) site usage and transcriptomic profiling of the cpsf30 mutant seedlings at 22°C and 28°C (Supplemental Figure 2A; Supplemental Table 1). Similarly, in the PAT-seq analysis, over 1000 switch genes were found in the cpsf30 mutant (Figure 6C), and over 50% of these switch genes were overlapped with those in the cpsf100 mutant (Supplemental Figure 18), suggesting that CPSF30 and CPSF100 may cooperatively regulate APA during thermomorphogenesis. In addition, 49.8% of switch genes in cpsf30 and 46% of switch genes in cpsf100 overlapped with switch genes in siz1-2 mutant, respectively (Supplemental Figure 18). Consistently, the depletion of CPSF30 promoted the relative expression of proximal transcripts in ELF3, YUC8, PIF4, and distal transcripts in ELF4 in response to warm temperatures (Figure 6D). CPSF30-M or CPSF30-L but not CPSF30-S compensated for the APA usage of the above genes in the cpsf30 mutant (Supplemental Figure 19). We further found that the overexpression of CPSF30-M/L, not

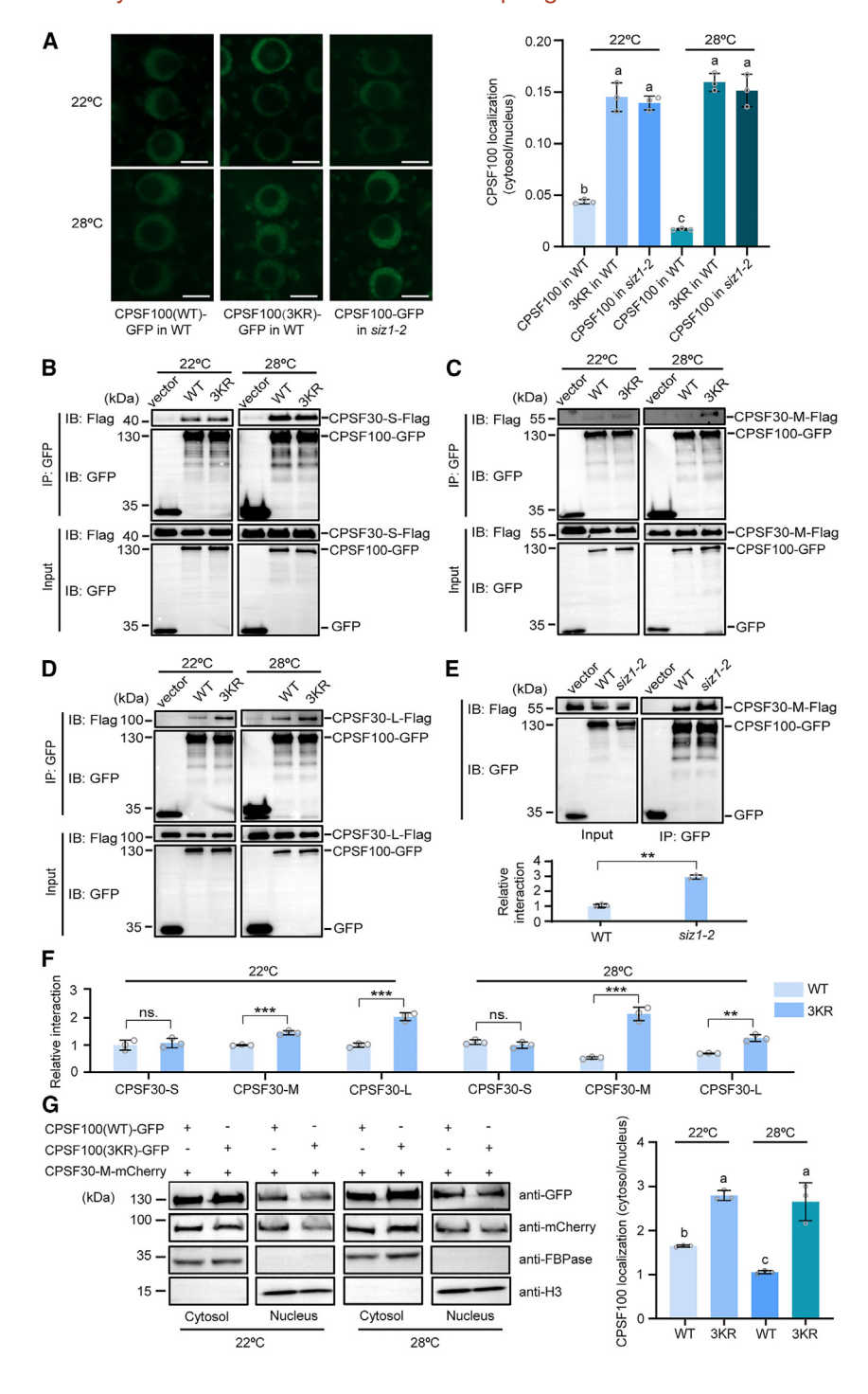


Figure 5. SUMOylation of CPSF100 suppresses its interaction with CPSF30 isoforms.

(A) The effect of SUMOylation on the subcellular localization of CPSF100-GFP in Arabidopsis. The representative GFP signals of CPSF100(WT)-GFP and CPSF100(3KR)-GFP in complementary lines, as well as CPSF100(WT)-GFP in  $\it siz1-2$  at  $22^{\circ}C$  or  $28^{\circ}C$  are shown in the left graph. Scale bars, 5  $\mu m$ . Three biologically independent experiments showed similar patterns. The quantification data presented in the right graph for the cytosol/nucleus ratio of CPSF100 localization are mean  $\pm$  SD from five roots of each type of seedlings.

(B-F) Effect of CPSF100 SUMOylation on its interaction with CPSF30-S, CPSF30-M, or CPSF30-L in a Co-IP assay. The WT or 3KR version of CPSF100-GFP was co-expressed with FLAG-tagged CPSF30 isoforms in WT protoplasts overnight at 22°C or 28°C; CPSF100-GFP was coexpressed with FLAG-tagged CPSF30-M in WT and siz1-2 protoplasts overnight at 28°C. The protoplasts were collected for protein extraction, followed by Co-IP using anti-GFP beads. The input and IP samples were analyzed by immunoblots using anti-GFP and anti-FLAG antibodies. The representative images are shown in (B)-(E). Quantification data for the relative interaction intensity (the IP/input ratio of CPSF30 isoforms) are shown in (F) and the bottom graph of (E). Data are mean ± SD from three biologically independent experiments, and significant difference was analyzed via Student's t test (\*\*p < 0.01; \*\*\*p < 0.001; ns., p > 0.05).

**(G)** The distribution of CPSF100-GFP in the cytoplasmic and nuclear fractions. The indicated pairs of proteins were co-expressed in *N. benthamiana* leaves for 36 h, and then the leaves were treated at  $28^{\circ}\text{C}$  or  $22^{\circ}\text{C}$  for 12 h before collection for nuclear and cytoplasmic fractionation. Anti-FBPase and anti-H3 anti-bodies were used as markers for the cytoplasmic and nuclear fractions, respectively. The quantitative data of relative localization of CPSF100 (cytosol/nucleus) are mean  $\pm$  SD from three biologically independent experiments, and significant difference was analyzed via one-way ANOVA followed by Tukey's multiple comparison tests (p < 0.05).

CPSF30-S, was able to complement the relative expression of proximal/distal ELF3 and PIF4 transcripts in cpsf100 mutant (Supplemental Figure 20), supporting the functional association between CPSF100 and CPSF30 for APA regulation in this process. The frequency of U nucleotide usage in FUEs and U/A nucleotide usage in NUEs in CPSF30-regulated PACs was higher than that in common PACs (Figure 6E). Accordingly, more U-rich motifs in FUEs and more AAUAAA and its 1-nt variants in NUEs were used in CPSF30-regulated PACs than in common PACs (Figure 6F)

and 6G). These results suggested that CPSF30 alters APA by modulating the usage of poly(A) signals in thermomorphogenesis.

#### **DISCUSSION**

APA is an important pathway in the precise modulation of plasticity in gene expression (Guo and Lin, 2023; Wu et al., 2023), but its function and regulation mechanism in plants' responses to warm ambient temperatures are unclear. Here, we

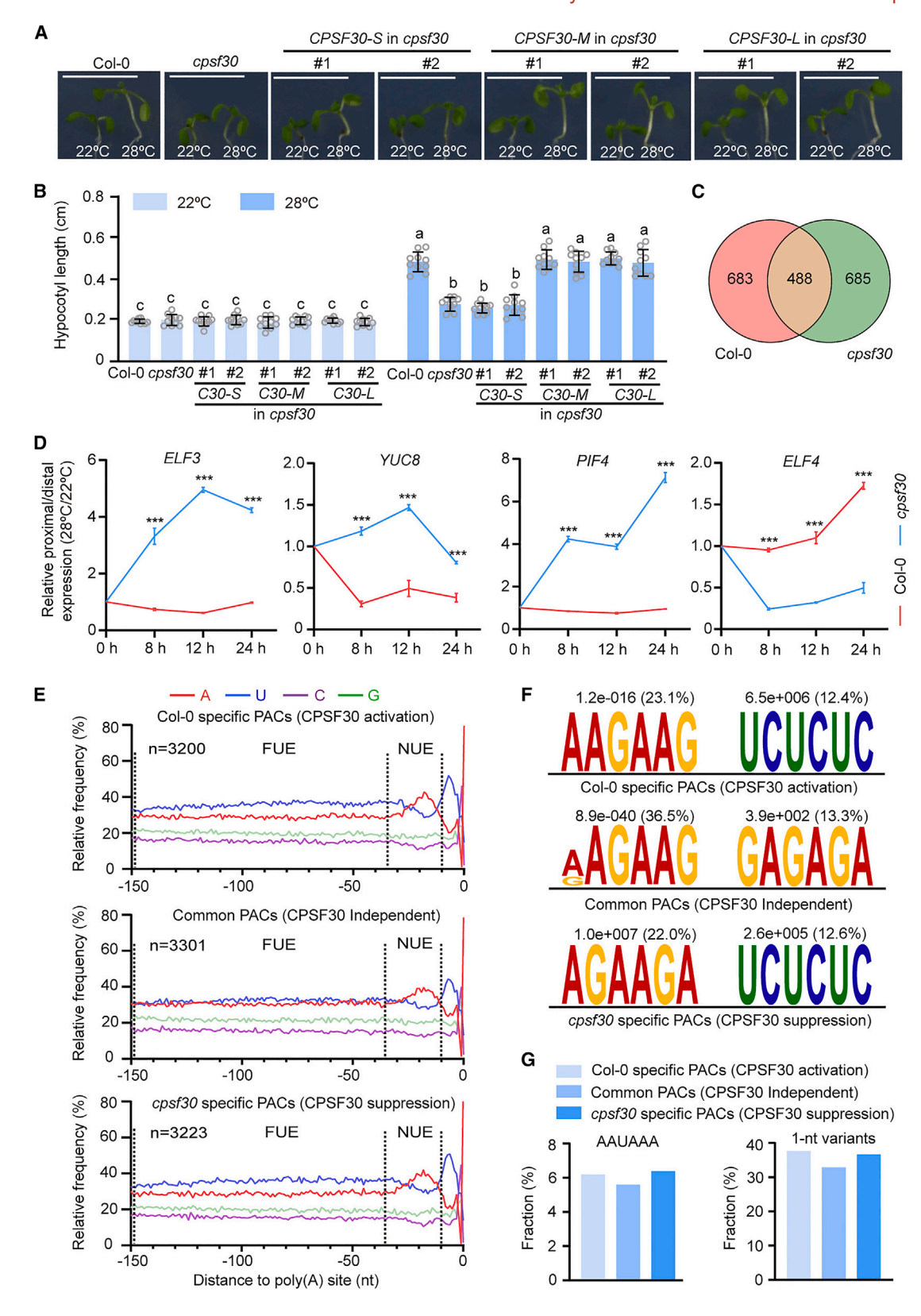


Figure 6. CPSF30 modulates global poly(A) site usage in thermomorphogenesis.

(A and B) Four-day-old seedlings of the indicated genotypes grown at 22°C were transferred to 22°C or 28°C for an additional 4 days before being photographed. The representative images are shown in (A); scale bars, 1 cm. The statistical analysis of hypocotyl lengths is shown in (B). Data are uncovered a mechanism that the SIZ1-mediated SUMOylation of CPSF100 restrains its interaction with CPSF30 to control the poly(A) site choice of downstream genes in plant thermomorphogenesis.

Our PAT-seq data uncovered the genome-wide profiling of poly(A) site usage in the WT, siz1-2, cpsf100, and cpsf30 mutant at 22°C and 28°C, and high overlapping percentages of these switch genes were found among these mutants. Compared to common PACs, the proteins of the above mutant-mediated PACs use more AAUAAA signals in NUEs and more U-rich signals in FUEs in response to warm temperatures, but other APA factors involved in this process need to be identified further (Forbes et al., 2006; Martin et al., 2012). Combined with the above evidence, the similar phenotypes of cpsf100 and cpsf30 mutants in thermoresponsive hypocotyl elongation supported their cooperation in the polyadenylation regulation of genes associated with warm temperature response, such as ELF3, YUC8, PIF4, and ELF4, in this situation.

Proteomic data showed that extreme HS increases SUMOylation of proteins involved in RNA processing (Miller et al., 2013), but targeting of SUMO on polyadenylation factors has not been reported in plants. Here, we identified CPSF100 as a SUMOylation substrate, and its SUMOylation was enhanced under warm temperatures in a SIZ1dependent manner. Consistently, previous research has demonstrated that SIZ1, but not another SUMO ligase MMS21, is responsible for mediating SUMOylation in response to high temperatures (Rytz et al., 2018). The small population of SUMOylated CPSF100 retained in the siz1-2 null mutant may be attributed to the conjugation mediated by E2. A previous study indicated that overexpression of CSPF30 results in the translocation of CPSF100 from the nucleus into the cytoplasm (Rao et al., 2009). Our data showed that SUMOylation of CPSF100 attenuates its association with CPSF30-L and CPSF30-M, resulting in increased accumulation of CPSF100 in the nucleus, where the CPSF complex recognizes nascent RNAs for polyadenylation. This notion was supported by our poly(A) signal usage data of the 3KR version of CPSF100 complementary plants. Given that 28°C induces SUMOylation of CPSF100, the nuclear CPSF complex may be dynamically regulated in this manner during warm temperature responses in plants. Interestingly, CPSF30-S also interacts with CPSF100 for its translocation (Rao et al., 2009; Zhao et al., 2009), suggesting that the N-terminal of CPSF30 contributes to its interaction with CPSF100, but the effect of CPSF100 SU-MOylation on this association requires the C-terminal. The effect of CPSF100 SUMOylation on its interaction with CPSF30-M or CPSF30-L may change the accumulation levels of CPSF100 and CPSF30 in the nucleus and alter the choice of poly(A) site. This is consistent with the finding in mammals that different levels of poly(A) factor affect the choice of APA (Shi, 2012; Tang and Zhou, 2022). However, the mechanism of domain specificity of this regulation in APA needs further investigation.

As a model, under warm temperatures, the SIZ1-mediated SUMOylation of CPSF100 is upregulated to suppress its association with CPSF30-M/L, resulting in an increase in CPSF100 accumulation in the nucleus, thereby altering the poly(A) site usage of downstream genes required for hypocotyl growth in warm temperature responses (Figure 7). Our current work will provide clues for further studies in other species and the improvement of stress tolerance in crops.

#### **MATERIALS AND METHODS**

#### Plant materials and growth conditions

The plant materials used in this study were Arabidopsis thaliana (L.) Heynhold. The seeds of siz1-2 (SALK\_065397 in the ecotype Col-0 background) and cpsf30 (SALK\_049389 in the ecotype Col-0 background) were obtained from the Arabidopsis Biological Resource Center (ABRC). The seeds of esp5-1 (designated as cpsf100 in this study, an amino acid substitution [G to E] at the 12th position of CPSF100 in the ecotype C24 background) and its control plants (with construct amp311 in the ecotype C24 background, designated as WT in the experiment sets with cpsf100 study) were described previously (Herr et al., 2006). Seeds were surface sterilized for 5 min in 2.5% (v/v) NaClO solution, rinsed 5 times with sterile water, and plated on Murashige and Skoog medium with 1.5% (w/v) sucrose, 0.8% (w/v) agar, 0.05% MES, and pH 5.7-5.8, and then synchronized at 4°C for 3 days in the dark. Plants were grown under long-day conditions (16 h light/8 h dark) at 22°C. For hypocotyl growth analysis, plants were grown for 4 days at 22°C before the transfer to 28°C for an additional 4 days.

#### Generation of transgenic plants

To generate the *CPSF100* complementation plants, the genomic DNA of *CPSF100* with the upstream 2000 bp from ATG as its promoter was cloned in pCambia1300-221 and then transformed into the *cpsf100* mutant background. The mutant version of the *CPSF100* construct was created by site-directed mutagenesis. To generate the *CPSF30* complementation plants, the coding sequences (CDS) of *CPSF30-S*, *CPSF30-L*, or *CPSF30-M* with the upstream 2000 bp from ATG as its promoter was cloned in pCambia1300-221 and then transformed into the *cpsf30* mutant background. To generate transgenic plants overexpressing *CPSF100* in *siz1-2* mutant background, the CDS of *CPSF100* was cloned into pCambia-35S::GFP. To generate

mean  $\pm$  SD (n = 10) from one independent experiment. Three biologically independent experiments showed similar patterns. Significant difference was analyzed via one-way ANOVA followed by Tukey's multiple comparison tests (p < 0.05). C30-S, CPSF30-S; C30-M, CPSF30-M; C30-L, CPSF30-L. (C) The Venn diagram showing the overlap of switch genes in response to warm temperatures between Col-0 and cpsf30 plants. p < 0.05 was considered

(C) The Venn diagram showing the overlap of switch genes in response to warm temperatures between Col-0 and cpsf30 plants. p < 0.05 was considered statistically significant for poly(A) sites' usage of switch genes.

(D) qRT-PCR analysis for the relative expression ratio of APA transcripts of *ELF3*, *YUC8*, *PIF4*, and *ELF4* in Col-0 and *cpsf30*. The relative expression of different transcripts was defined as the ratio of proximal transcript expression/distal transcript expression (28°C/22°C); the detailed calculation is included in Materials and methods. Data are mean  $\pm$  SD from three technological replicates in a single experiment. Three biologically independent experiments showed similar patterns. Significant difference between different samples at the same time point was analyzed using Student's t test (\*\*\*p < 0.001).

(E-G) Position-by-position analysis of average base composition at 150 nt upstream of poly(A) sites, including FUEs and NUEs, are shown in (E). The poly(A) signal motifs in FUEs are shown in (F). The AAUAAA signal usage and 1-nt variants of AAUAAA signal usage in NUEs are shown in (G).

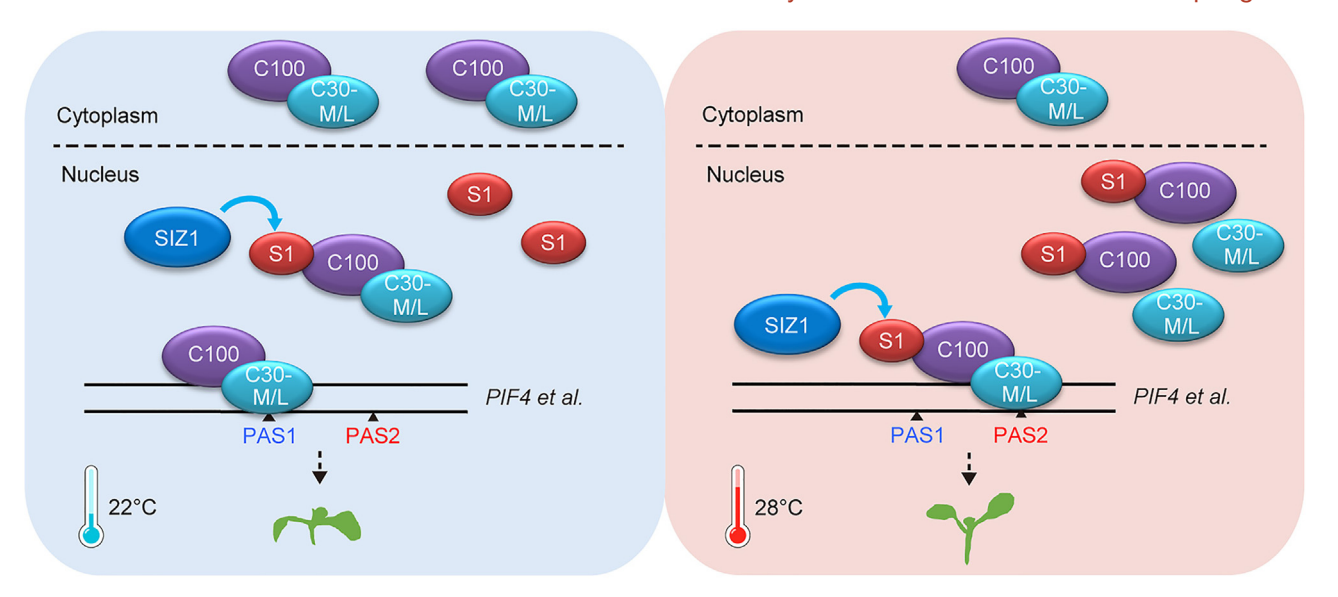


Figure 7. A proposed model for SIZ1-mediated SUMOylation of CPSF100 in the regulation of thermomorphogenesis in plants.

Under warm temperatures, there is an upregulation of SIZ1-mediated SUMOylation of CPSF100, leading to the suppression of its association with CPSF30-M/L. This results in an increase in the accumulation of CPSF100 in the nucleus, thereby causing alterations in the poly(A) site usage of downstream genes associated with hypocotyl growth in warm temperature responses. S1, SUMO1; C100, CPSF100; C30-M/L, CPSF30-M/L; PAS, Poly(A) site.

plants overexpressing *proximal* or *distal PIF4* in Col-0, the proximal or distal version of *PIF4* was cloned to the pCambia vector with a *UBQ10* promoter. Transgenic plants were generated by Agrobacterium-mediated transformation by the floral-dip method (Clough and Bent, 1998).

#### **SUMOylation assays**

The *in vitro* SUMOylation assay in *Escherichia coli* was carried out as previously described (Okada et al., 2009). The CDS of CPSF subunits with a FLAG tag were respectively cloned into the pCDFDuet-1 vector and then transformed for expression in the bacteria carrying pET28-SAE1a- $His_6$ -AtSAE2 (E1) with pACYCDuet-1-SU-MO1GG or pACYCDuet-1-SCE1-SUMO1GG. After 0.5 mM isopropyl  $\beta$ -d-1-thiogalactopyranoside induction at  $28^{\circ}$ C for 14 h, the cells were harvested for immunoblotting using an anti-FLAG antibody (CW0287; Cwbio).

The *in vivo* SUMOylation assay was accomplished as previously described with modifications (Niu et al., 2019). Myc-SUMO1GG was coexpressed with CPSF100-GFP (WT), or CPSF100-GFP (3KR) in the WT or *siz1-2* protoplasts. After 14 h culture at 22°C or 28°C, cells were harvested and extracted in an extraction buffer containing 50 mM Tris-HCl (pH 7.5), 150 mM NaCl, 1 mM MgCl<sub>2</sub>, 20% (v/v) glycerol, 0.2% (v/v) Nonidet P-40, 20 mM *N*-ethylmaleimide, and 1× protease inhibitor cocktail (Roche). The protein extracts were incubated with anti-GFP affinity beads at 4°C for 2 h. The protein samples were subjected to immunoblotting using anti-GFP and anti-Myc antibodies.

For detecting the SUMOylation of total proteins, the WT and *siz1-2* seed-lings were initially grown at 22°C for 5 days and then transferred to 28°C (28°C treatment) or kept at 22°C (22°C treatment) for an additional 1 or 4 days. The protein samples were subjected to immunoblotting using an anti-SUMO1 antibody (Abcam, ab5316).

#### Co-IP assay

To analyze the effect of CPSF100 SUMOylation on its interaction with CPSF30-S, CPSF30-M, or CPSF30-L, Co-IP assays were performed as described previously (Wang et al., 2020). Total proteins were extracted

in the Co-IP lysis buffer (50 mM Tris-HCl, pH 7.5, 150 mM NaCl, 1 mM MgCl $_2$ , 20% [v/v] glycerol, 0.2% [v/v] Nonidet P-40, and 1× protease inhibitor cocktail [Roche]). The protein supernatant was collected after centrifugation at 13 000 × g for 15 min, and incubated with anti-GFP affinity beads at 4°C for 2 h. Then, the GFP affinity beads were rinsed 3 times with a washing buffer (50 mM Tris-HCl, pH 7.4, 150 mM NaCl, 1 mM MgCl $_2$ , 20% [v/v] glycerol, and 0.02% [v/v] Nonidet P-40). The input and IP samples were analyzed by immunoblots using anti-GFP and anti-FLAG antibodies.

#### **Nuclear extraction and fractionation**

To isolate nuclei, leaves of *N. benthamiana* plants were ground in liquid nitrogen and homogenized in nuclei isolation buffer (50 mM Tris-HCl, pH 7.4, 150 mM KCl, 250 mM sucrose, 25% [v/v ] glycerol, 1 mM EDTA, 2.5 mM MgCl<sub>2</sub>, 30 mM  $\beta$ -mercaptoethanol) containing 50  $\mu$ M MG132 (Sigma) and 1× protease inhibitor cocktail (Roche). The homogenate was centrifuged at 3000 × g for 5 min at 4°C. The supernatant was saved as the cytosolic fraction; the pellet was rinsed with nuclei wash buffer (50 mM Tris-HCl, pH 7.4, 25% [v/v] glycerol, 2.5 mM MgCl<sub>2</sub>), resuspended with plant protein extraction buffer with 1% (v/v) Triton X-100, and saved as the nuclear fraction.

#### LCI assay

The CDS of the WT or 3KR version of *CPSF100* was cloned into pCAMBIA-1300-*cLUC*, and the CDS of *CPSF30-M/L* was cloned into pCAMBIA-1300-*nLUC*. Then, the indicated protein pairs were expressed in *N. benthamiana* leaves via Agrobacterium-mediated infiltration. After growing at 25°C for 36 h, the plants were transferred to 22°C or 28°C for 12 h. The leaves were infiltrated with d-luciferin (Macklin), and luminescence was detected using a low-light cooled charge-coupled device imaging system (Tanon).

#### **Dual-luciferase reporter assay**

A dual-LUC assay was employed to assess the impact of the candidate protein on the expression of a target gene. The dual-LUC reporter contains a renilla LUC (REN) and a LUC (Hellens et al., 2005). To study the effect of the proximal and distal transcripts of *ELF3* on the *YUC8* promoter activity, the *YUC8* promoter (a 2000-bp fragment upstream from

#### SUMOylation controls APA in thermomorphogenesis

the start codon) was cloned to pGreenII0800-LUC to generate the reporter construct. The pGREEN0800-LUC vector also contains the REN gene driven by a 35S promoter. The reporter construct was cotransformed with proximal ELF3-GFP or distal ELF3-GFP into protoplasts for the dual-LUC assay. The GFP vector was used in a control sample. The activity of YUC8 promoter was analyzed using the ratio of LUC/REN.

#### PAT-seq library preparation and sequencing

For the construction of PAT-seq libraries, three independent biological replicates were included. Seedlings were initially grown at 22°C for 5 days and then transferred to 28°C (28°C treatment) or kept at 22°C (22°C treatment) for 1 day. Total RNA was isolated using the TRIzol reagent (Invitrogen), and DNase I (Takara) was used to remove DNA, followed by a column-based RNA purification. The quality and concentration of total RNA were tested by DNA agarose gel electrophoresis and NanoDrop 2000. Then, 2 µg high-quality total RNA was used to construct PAT-seq libraries as described previously (Lin et al., 2021). Briefly, RNA was fragmented in 5× first-strand buffer (Invitrogen) at 94°C for 4 min. RNA fragments with poly(A) tails were enriched via oligo(dT)<sub>25</sub> magnetic beads (New England Biolabs). RT-PCR was performed using oligo(dT)<sub>18</sub> primers with the SMARTScribe enzyme (Clontech) for 2 h at 42°C, and a 5' adapter with a last nucleic acid locked modification for template switching was added for an additional 2 h at 42°C to obtain cDNA. Then, cDNA was purified by AMPURE XP beads (Vazyme). Ten PCR cycles with KAPA HiFi were performed with cDNA as a template to produce the first PCR products, followed by purification using AMPURE XP beads. Eight PCR cycles with KAPA HiFi were performed with the purified first PCR products as templates to produce the PAT-seq library. The library was run on a 2% agarose gel, and 300- to 500-bp library fragments were purified. Libraries were qualified and quantified by Agilent Bioanalyzer 2100, Qubit 2.0, and qRT-PCR. Finally, libraries were sequenced on the HiSeq X Ten platform.

#### Raw data processing

The raw data were processed according to previously described methods (Wu et al., 2011; Ye et al., 2021). Briefly, raw data were processed with FASTX Toolkit to remove low-quality reads (version 0.0.14, parameters, fastq\_quality\_filter with -q 10 -p 50 -v -Q 33). Then, valid reads with poly(T) with length ≥25 nt were obtained with a customized Perl script findTailAT.pl from the PlantAPAdb website (http://www.bmibig.cn/plantAPAdb). Valid reads with poly(T) were mapped to the Arabidopsis reference genome (The Arabidopsis Information Resource 10th annotation; www.Arabidopsis.org) using Bowtie2 software (version 2.1.0, parameters "-L 25, -N 0, -i S,1,1.15-no-unal"). Finally, the precise locations of poly(A) sites were parsed from these valid mapping records using a customized Perl script parseSAM2PAT.pl from the PlantAPAdb website, and identical sites were aggregated in each sample using bedtools (bedtools with groupby, -g 1,6,2, -c 1, and -o count).

#### APA dynamics identification

As poly(A) site microheterogeneity is pervasive in plants, a weighted density peak clustering model was used to analyze APA dynamics according to previously described methods (Ye et al., 2021). p Values were averaged to estimate the significance of difference (p <0.05 for the significance cutoff).

The DESeq2 package (version 1.26.0) was used to normalize reads and compare differential expression poly(A) sites and genes between WT and mutant. An adjusted  $\rho$  value < 0.05 was considered as statistical significance for poly(A) sites and genes.

#### **GO** enrichment

Switch genes were submitted to Agrigo2 (http://systemsbiology.cau.edu. cn/agriGOv2/) for GO enrichment. Singular enrichment analyses were chosen and The Arabidopsis Information Resource 10th annotation acted as the background. The false discovery rate corrected p < 0.05 was used as a cutoff for statistical significance.

#### Poly(A) signal analyses

The sequences surrounding poly(A) sites ranging from -300 to +100 nt were extracted for single-nucleotide profile analysis, as reported previously by Loke et al. (2005). Transcripts used for poly(A) signals analysis were extracted from switch genes containing PACs. We focused on NUE regions between -10 and -35 nt upstream of poly(A) sites. The canonical AAUAAA signal and its 1-nt variants were analyzed as described previously (Loke et al., 2005). 1-nt variants of AAUAAA contained 18 hexamers (UAUAAA, CAUAAA, GAUAAA, AUUAAA, ACUAAA, AGUAAA, AAUAAA, AACAAA, AACAAA, AAGAAA, AAUAAA, AAUCAA, AAUGAA, AAUGAA, AAUAAA, AAUAAA, AAUAAA, AAUAAA, AAUAAA, AAUAAA, AAUAAA, AAUAAA, AAUAAA, ABUAAA, ABUAAA, BE m for Motif Elicitation (MEME) was used to enrich poly(A) signals in FUE regions (-150 to -35 nt from the poly(A) site) (Bailey et al., 2009; Martin et al., 2012).

#### qRT-PCR analysis

For verification of the expression of poly(A) sites, approximately 1  $\mu$ g high-quality total RNA was reverse transcribed with oligo(dT)<sub>18</sub> primers by the reverse transcriptase. RNA from 7-day-old seedlings was isolated. qRT-PCR assays were performed using the CFX96TM real-time PCR detection system (Bio-Rad) with SYBR Premix Ex TaqII fluorescent dye. *ACTIN2* was used as an internal control. All primer sequences used in this study are listed in Supplemental Table 2.

For measuring the proximal/distal expression, the relative expression of indicated transcripts at each time point (8, 12, and 24 h) was calculated as the ratio of 28°C/22°C. After being normalized with the expression of the indicated transcript in the WT sample (0 h), the relative ratio shown in the figures was calculated as the ratio of the relative expression of proximal transcript (28°C/22°C) to distal transcript (28°C/22°C).

#### DATA AND CODE AVAILABILITY

The accession numbers of the genes in this study are as follows: *SIZ1* (AT5G60410), *CPSF100* (AT5G23880), *CPSF30* (AT1G30460), *ELF3* (AT2G25930), *YUC8* (AT4G28720), *PIF4* (AT2G43010), *ELF4* (AT2G40080), *SUMO1* (AT4G26840), *SAE1a* (AT4G24940), *SAE2* (AT2G21470), *SCE1* (AT3G57870), *FY* (AT5G13480), *CPSF73I* (AT1G61010), *CPSF73II* (AT2G0 1730), and *ACTIN2* (AT3G18780).

All PAT-seq raw data for this study are available at the NCBI website under accession number PRJNA970088.

#### **FUNDING**

The project was supported by grants from the Major Program of Guangdong Basic and Applied Research (2019B030302006), the National Natural Science Foundation of China (32000449, 32270292, 32270344, 32270752, and 32170593), the China Postdoctoral Science Foundation (2020M672674), the Program for Changjiang Scholars, the Natural Science Foundation of Guangdong Province, China (2024A1515011497, 2020B1515020007, and 2024A1515011071), the Guangdong Provincial Pearl River Talent Plan (2019QN01N108), and the National Science Foundation of USA (2347540).

#### **ACKNOWLEDGMENTS**

We thank Prof. Andreas Bachmair for providing the SUMO E1 plasmid and ABRC for the Arabidopsis seeds used in this study. We thank other lab

#### **Molecular Plant**

members for helpful discussions and sharing protocols. No conflict of interest declared.

#### **AUTHOR CONTRIBUTIONS**

C.Y., J.L., and Q.Q.L. designed the experiments and supervised the research. Z.Y. and J.W. conducted the experiments. C.Z., Q.Z., L.S., B.S., D.H., J.J., J.H., X.O., and Z.Z. provided technological support. Z.Y., J.W., J.L., C.Y., and Q.Q.L. analyzed the data and wrote the manuscript. All authors read and approved this manuscript.

#### SUPPLEMENTAL INFORMATION

Supplemental information is available at Molecular Plant Online.

Received: January 27, 2024 Revised: July 1, 2024 Accepted: July 23, 2024

#### **REFERENCES**

- Bailey, T.L., Boden, M., Buske, F.A., Frith, M., Grant, C.E., Clementi, L., Ren, J., Li, W.W., and Noble, W.S. (2009). MEME SUITE: tools for motif discovery and searching. Nucleic Acids Res. 37:W202–W208. https://doi.org/10.1093/nar/gkp335.
- Casal, J.J., and Balasubramanian, S. (2019). Thermomorphogenesis. Annu. Rev. Plant Biol. 70:321–346. https://doi.org/10.1146/annurev-arplant-050718-095919.
- Clough, S.J., and Bent, A.F. (1998). Floral dip: a simplified method for *Agrobacterium*-mediated transformation of *Arabidopsis thaliana*. Plant J. **16**:735–743. https://doi.org/10.1046/j.1365-313x.1998. 00343.x.
- Conesa, C.M., Saez, A., Navarro-Neila, S., de Lorenzo, L., Hunt, A.G., Sepúlveda, E.B., Baigorri, R., Garcia-Mina, J.M., Zamarreño, A.M., Sacristán, S., et al. (2020). Alternative Polyadenylation and Salicylic Acid Modulate Root Responses to Low Nitrogen Availability. Plants (Basel) 9:251. https://doi.org/10.3390/plants 9020251.
- Deng, X., and Cao, X. (2017). Roles of pre-mRNA splicing and polyadenylation in plant development. Curr. Opin. Plant Biol. 35:45–53. https://doi.org/10.1016/j.pbi.2016.11.003.
- Forbes, K.P., Addepalli, B., and Hunt, A.G. (2006). An Arabidopsis Fip1 homolog interacts with RNA and provides conceptual links with a number of other polyadenylation factor subunits. J. Biol. Chem. 281:176–186. https://doi.org/10.1074/jbc.M510964200.
- Fu, H., Yang, D., Su, W., Ma, L., Shen, Y., Ji, G., Ye, X., Wu, X., and Li, Q.Q. (2016). Genome-wide dynamics of alternative polyadenylation in rice. Genome Res. 26:1753–1760. https://doi.org/10.1101/gr. 210757.116.
- Fu, H., Wang, P., Wu, X., Zhou, X., Ji, G., Shen, Y., Gao, Y., Li, Q.Q., and Liang, J. (2019). Distinct genome-wide alternative polyadenylation during the response to silicon availability in the marine diatom *Thalassiosira pseudonana*. Plant J. 99:67–80. https://doi.org/10.1111/ tpj.14309.
- Guo, S., and Lin, S. (2023). mRNA alternative polyadenylation (APA) in regulation of gene expression and diseases. Genes Dis. 10:165–174. https://doi.org/10.1016/j.gendis.2021.09.005.
- Hammoudi, V., Fokkens, L., Beerens, B., Vlachakis, G., Chatterjee, S., Arroyo-Mateos, M., Wackers, P.F.K., Jonker, M.J., and van den Burg, H.A. (2018). The Arabidopsis SUMO E3 ligase SIZ1 mediates the temperature dependent trade-off between plant immunity and growth. PLoS Genet. 14:e1007157. https://doi.org/10.1371/journal. pgen.1007157.

#### SUMOvlation controls APA in thermomorphogenesis

- Han, D., Yu, Z., Lai, J., and Yang, C. (2022). Post-translational modification: a strategic response to high temperature in plants. aBIOTECH 3:49–64. https://doi.org/10.1007/s42994-021-00067-w.
- Hedhly, A., Hormaza, J.I., and Herrero, M. (2009). Global warming and sexual plant reproduction. Trends Plant Sci. 14:30–36. https://doi. org/10.1016/j.tplants.2008.11.001.
- Hellens, R.P., Allan, A.C., Friel, E.N., Bolitho, K., Grafton, K., Templeton, M.D., Karunairetnam, S., Gleave, A.P., and Laing, W.A. (2005). Transient expression vectors for functional genomics, quantification of promoter activity and RNA silencing in plants. Plant Methods 1:13. https://doi.org/10.1186/1746-4811-1-13.
- Herr, A.J., Molnàr, A., Jones, A., and Baulcombe, D.C. (2006). Defective RNA processing enhances RNA silencing and influences flowering of Arabidopsis. Proc. Natl. Acad. Sci. USA 103:14994–15001. https://doi.org/10.1073/pnas.0606536103.
- Hou, Y., Yan, Y., and Cao, X. (2022). Epigenetic regulation of thermomorphogenesis in *Arabidopsis thaliana*. aBIOTECH 3:12–24. https://doi.org/10.1007/s42994-022-00070-9.
- Huang, J., Huang, J., Feng, Q., Shi, Y., Wang, F., Zheng, K., Huang, Q., Jiang, J., Luo, S., Xie, Y., et al. (2023). SUMOylation facilitates the assembly of a Nuclear Factor-Y complex to enhance thermotolerance in Arabidopsis. J. Integr. Plant Biol. 65:692–702. https://doi.org/10.1111/jipb.13396.
- Hunt, A.G. (2020). mRNA 3' end formation in plants: Novel connections to growth, development and environmental responses. Wiley Interdiscip. Rev. RNA 11:e1575. https://doi.org/10.1002/wrna.1575.
- Kim, M., Swenson, J., McLoughlin, F., and Vierling, E. (2023). Mutation of the polyadenylation complex subunit CstF77 reveals that mRNA 3' end formation and HSP101 levels are critical for a robust heat stress response. Plant Cell 35:924–941. https://doi.org/10.1093/plcell/ koac351.
- Koini, M.A., Alvey, L., Allen, T., Tilley, C.A., Harberd, N.P., Whitelam, G.C., and Franklin, K.A. (2009). High temperature-mediated adaptations in plant architecture require the bHLH transcription factor PIF4. Curr. Biol. 19:408–413. https://doi.org/10.1016/j.cub. 2009.01.046.
- Kumar, S.V., Lucyshyn, D., Jaeger, K.E., Alós, E., Alvey, E., Harberd, N.P., and Wigge, P.A. (2012). Transcription factor PIF4 controls the thermosensory activation of flowering. Nature 484:242–245. https:// doi.org/10.1038/nature10928.
- Kurepa, J., Walker, J.M., Smalle, J., Gosink, M.M., Davis, S.J., Durham, T.L., Sung, D.Y., and Vierstra, R.D. (2003). The small ubiquitin-like modifier (SUMO) protein modification system in Arabidopsis. Accumulation of SUMO1 and -2 conjugates is increased by stress. J. Biol. Chem. 278:6862–6872. https://doi.org/10.1074/jbc. M209694200.
- Li, Y., Williams, B., and Dickman, M. (2017). Arabidopsis B-cell lymphoma2 (Bcl-2)-associated athanogene 7 (BAG7)-mediated heat tolerance requires translocation, sumoylation and binding to WRKY29. New Phytol. 214:695–705. https://doi.org/10.1111/nph. 14388.
- Lin, J., and Li, Q.Q. (2023). Coupling epigenetics and RNA polyadenylation: missing links. Trends Plant Sci. 28:223–234. https://doi.org/10.1016/j.tplants.2022.08.023.
- Lin, J., Ye, C., and Li, Q.Q. (2021). QPAT-seq, a rapid and deduplicatable method for quantification of poly(A) site usages. Methods Enzymol. 655:73–83. https://doi.org/10.1016/bs.mie.2021. 04.002.
- Lin, J., Xu, R., Wu, X., Shen, Y., and Li, Q.Q. (2017). Role of cleavage and polyadenylation specificity factor 100: anchoring poly(A) sites and modulating transcription termination. Plant J. 91:829–839. https://doi.org/10.1111/tpj.13611.
- **1404** Molecular Plant 17, 1392–1406, September 2 2024 © 2024 The Author.

- Loke, J.C., Stahlberg, E.A., Strenski, D.G., Haas, B.J., Wood, P.C., and Li, Q.Q. (2005). Compilation of mRNA polyadenylation signals in Arabidopsis revealed a new signal element and potential secondary structures. Plant Physiol. 138:1457–1468. https://doi.org/10.1104/pp. 105.060541.
- Martin, G., Gruber, A.R., Keller, W., and Zavolan, M. (2012). Genome-wide analysis of pre-mRNA 3' end processing reveals a decisive role of human cleavage factor I in the regulation of 3' UTR length. Cell Rep. 1:753-763. https://doi.org/10.1016/j.celrep. 2012.05.003.
- Miller, M.J., Scalf, M., Rytz, T.C., Hubler, S.L., Smith, L.M., and Vierstra, R.D. (2013). Quantitative proteomics reveals factors regulating RNA biology as dynamic targets of stress-induced SUMOylation in Arabidopsis. Mol. Cell. Proteomics 12:449–463. https://doi.org/10.1074/mcp.M112.025056.
- Miura, K., Jin, J.B., and Hasegawa, P.M. (2007). Sumoylation, a post-translational regulatory process in plants. Curr. Opin. Plant Biol. 10:495–502. https://doi.org/10.1016/j.pbi.2007.07.002.
- Niu, D., Lin, X.L., Kong, X., Qu, G.P., Cai, B., Lee, J., and Jin, J.B. (2019).
  SIZ1-Mediated SUMOylation of TPR1 Suppresses Plant Immunity in Arabidopsis. Mol. Plant 12:215–228. https://doi.org/10.1016/j.molp. 2018.12.002.
- Okada, S., Nagabuchi, M., Takamura, Y., Nakagawa, T., Shinmyozu, K., Nakayama, J.i., and Tanaka, K. (2009). Reconstitution of Arabidopsis thaliana SUMO pathways in E. coli: functional evaluation of SUMO machinery proteins and mapping of SUMOylation sites by mass spectrometry. Plant Cell Physiol. 50:1049–1061. https://doi.org/10.1093/pcp/pcp056.
- Park, H.J., Kim, W.Y., Park, H.C., Lee, S.Y., Bohnert, H.J., and Yun, D.J. (2011). SUMO and SUMOylation in plants. Mol. Cells 32:305–316. https://doi.org/10.1007/s10059-011-0122-7.
- Quint, M., Delker, C., Franklin, K.A., Wigge, P.A., Halliday, K.J., and van Zanten, M. (2016). Molecular and genetic control of plant thermomorphogenesis. Nat. Plants 2:15190. https://doi.org/10.1038/ nplants.2015.190.
- Rao, S., Dinkins, R.D., and Hunt, A.G. (2009). Distinctive interactions of the Arabidopsis homolog of the 30 kD subunit of the cleavage and polyadenylation specificity factor (AtCPSF30) with other polyadenylation factor subunits. BMC Cell Biol. 10:51. https://doi. org/10.1186/1471-2121-10-51.
- Rytz, T.C., Miller, M.J., McLoughlin, F., Augustine, R.C., Marshall, R.S., Juan, Y.T., Charng, Y.Y., Scalf, M., Smith, L.M., and Vierstra, R.D. (2018). SUMOylome Profiling Reveals a Diverse Array of Nuclear Targets Modified by the SUMO Ligase SIZ1 during Heat Stress. Plant Cell 30:1077–1099. https://doi.org/10.1105/tpc.17.00993.
- Shi, Y. (2012). Alternative polyadenylation: new insights from global analyses. RNA 18:2105–2117. https://doi.org/10.1261/rna. 035899.112.
- Shi, Y., and Manley, J.L. (2015). The end of the message: multiple protein-RNA interactions define the mRNA polyadenylation site. Genes Dev. 29:889–897. https://doi.org/10.1101/gad.261974. 115.
- Song, P., Yang, J., Wang, C., Lu, Q., Shi, L., Tayier, S., and Jia, G. (2021).
  Arabidopsis N<sup>6</sup>-methyladenosine reader CPSF30-L recognizes FUE signals to control polyadenylation site choice in liquid-like nuclear bodies. Mol. Plant 14:571–587. https://doi.org/10.1016/j.molp.2021.
  01.014
- Sun, J., Qi, L., Li, Y., Chu, J., and Li, C. (2012). PIF4-mediated activation of YUCCA8 expression integrates temperature into the auxin pathway in regulating Arabidopsis hypocotyl growth. PLoS Genet. 8:e1002594. https://doi.org/10.1371/journal.pgen.1002594.

- Tang, P., and Zhou, Y. (2022). Alternative polyadenylation regulation: insights from sequential polyadenylation. Transcription 13:89–95. https://doi.org/10.1080/21541264.2022.2114776.
- Téllez-Robledo, B., Manzano, C., Saez, A., Navarro-Neila, S., Silva-Navas, J., de Lorenzo, L., González-García, M.P., Toribio, R., Hunt, A.G., Baigorri, R., et al. (2019). The polyadenylation factor FIP1 is important for plant development and root responses to abiotic stresses. Plant J. 99:1203–1219. https://doi.org/10.1111/tpj. 14416.
- **Thines, B., and Harmon, F.G.** (2010). Ambient temperature response establishes ELF3 as a required component of the core Arabidopsis circadian clock. Proc. Natl. Acad. Sci. USA **107**:3257–3262. https://doi.org/10.1073/pnas.0911006107.
- Thomas, P.E., Wu, X., Liu, M., Gaffney, B., Ji, G., Li, Q.Q., and Hunt, A.G. (2012). Genome-wide control of polyadenylation site choice by CPSF30 in Arabidopsis. Plant Cell 24:4376–4388. https://doi.org/10.1105/tpc.112.096107.
- Tian, B., and Manley, J.L. (2017). Alternative polyadenylation of mRNA precursors. Nat. Rev. Mol. Cell Biol. 18:18–30. https://doi.org/10.1038/nrm.2016.116.
- Tian, Y.Y., Li, W., Wang, M.J., Li, J.Y., Davis, S.J., and Liu, J.X. (2022).
  REVEILLE 7 inhibits the expression of the circadian clock gene *EARLY FLOWERING 4* to fine-tune hypocotyl growth in response to warm temperatures. J. Integr. Plant Biol. **64**:1310–1324. https://doi.org/10.1111/jipb.13284.
- Wang, F., Liu, Y., Shi, Y., Han, D., Wu, Y., Ye, W., Yang, H., Li, G., Cui, F., Wan, S., et al. (2020). SUMOylation Stabilizes the Transcription Factor DREB2A to Improve Plant Thermotolerance. Plant Physiol. 183:41–50. https://doi.org/10.1104/pp.20.00080.
- Wu, J., Ma, L., and Cao, Y. (2023). Alternative Polyadenylation Is a Novel Strategy for the Regulation of Gene Expression in Response to Stresses in Plants. Int. J. Mol. Sci. 24:4727. https://doi.org/10.3390/ ijms24054727.
- Wu, X., Wang, J., Wu, X., Hong, Y., and Li, Q.Q. (2020). Heat Shock Responsive Gene Expression Modulated by mRNA Poly(A) Tail Length. Front. Plant Sci. 11:1255. https://doi.org/10.3389/fpls.2020. 01255.
- Wu, X., Liu, M., Downie, B., Liang, C., Ji, G., Li, Q.Q., and Hunt, A.G. (2011). Genome-wide landscape of polyadenylation in Arabidopsis provides evidence for extensive alternative polyadenylation. Proc. Natl. Acad. Sci. USA 108:12533–12538. https://doi.org/10.1073/pnas.1019732108.
- Yan, C., Wang, Y., Lyu, T., Hu, Z., Ye, N., Liu, W., Li, J., Yao, X., and Yin, H. (2021). Alternative Polyadenylation in response to temperature stress contributes to gene regulation in *Populus trichocarpa*. BMC Genom. 22:53. https://doi.org/10.1186/s12864-020-07353-9.
- Ye, C., Zhou, Q., Wu, X., Ji, G., and Li, Q.Q. (2019). Genome-wide alternative polyadenylation dynamics in response to biotic and abiotic stresses in rice. Ecotoxicol. Environ. Saf. 183:109485. https:// doi.org/10.1016/j.ecoenv.2019.109485.
- Ye, C., Zhao, D., Ye, W., Wu, X., Ji, G., Li, Q.Q., and Lin, J. (2021). QuantifyPoly(A): reshaping alternative polyadenylation landscapes of eukaryotes with weighted density peak clustering. Brief. Bioinform. 22:bbab268. https://doi.org/10.1093/bib/bbab268.
- Yu, Z., Lin, J., and Li, Q.Q. (2019). Transcriptome Analyses of FY Mutants Reveal Its Role in mRNA Alternative Polyadenylation. Plant Cell 31:2332–2352. https://doi.org/10.1105/tpc.18.00545.
- Zhang, X., Huai, J., Liu, S., Jin, J.B., and Lin, R. (2020). SIZ1-Mediated SUMO Modification of SEUSS Regulates Photomorphogenesis in Arabidopsis. Plant Commun. 1:100080. https://doi.org/10.1016/j. xplc.2020.100080.

#### **Molecular Plant**

- Zhao, H., Xing, D., and Li, Q.Q. (2009). Unique features of plant cleavage and polyadenylation specificity factor revealed by proteomic studies. Plant Physiol. **151**:1546–1556. https://doi.org/10.1104/pp.109. 142729.
- $Zhao,\,Q.,\,Xie,\,Y.,\,Zheng,\,Y.,\,Jiang,\,S.,\,Liu,\,W.,\,Mu,\,W.,\,Liu,\,Z.,\,Zhao,\,Y.,$ Xue, Y., and Ren, J. (2014). GPS-SUMO: a tool for the prediction of

#### SUMOylation controls APA in thermomorphogenesis

- sumoylation sites and SUMO-interaction motifs. Nucleic Acids Res. 42:W325-W330. https://doi.org/10.1093/nar/gku383.
- Zheng, X.T., Wang, C., Lin, W., Lin, C., Han, D., Xie, Q., Lai, J., and Yang, C. (2022). Importation of chloroplast proteins under heat stress is facilitated by their SUMO conjugations. New Phytol. 235:173-187. https://doi.org/10.1111/nph.18121.